Biochar sorption of perfluoroalkyl substances (PFASs) in aqueous film-forming foams-impacted groundwater: effects of PFASs properties and groundwater chemistry

Hoang Nhat Phong Vo[1,2], Thi Minh Hong Nguyen[2], Huu Hao Ngo[1*], Wenshan Guo[1], Pradeep Shukla[2]

[1] *Centre for Technology in Water and Wastewater, School of Civil and Environmental Engineering, University of Technology Sydney, Sydney, NSW 2007, Australia*

[2] *Queensland Alliance for Environmental Health Sciences (QAEHS), The University of Queensland, 20 Cornwall Street, Woolloongabba, Queensland 4102, Australia*

***** Corresponding author: *E–mail address: ngohuuhao121@gmail.com*

Abstract

The widespread use of per- and polyfluoroalkyl substances (PFASs)-related products such as aqueous film-forming foams (AFFF) has led to increasing contamination of groundwater systems. The concentration of PFASs in AFFF-impacted groundwater can be several orders of magnitude higher than the drinking water standard. There is a need for a sustainable and effective sorbent to remove PFASs from groundwater. This work aims to investigate the sorption of PFASs in groundwater by biochar column. The specific objectives are to understand the influences of PFASs properties and groundwater chemistry to PFASs sorption by biochar. The PFASs-spiked Milli-Q water (including 19 PFASs) and four aqueous film-forming foams (AFFF)-impacted groundwater were used. The partitioning coefficients (log K_d) of long chain PFASs ranged from 0.77 to 4.63 while for short chain PFASs they remained below 0.68. For long chain PFASs ($C \geq 7$), log K_d increased by 0.5 and 0.8 for each CF_2 moiety of PFCAs and PFSAs, respectively. Dissolved organic matter (DOM) was the most influential factor in PFASs sorption over pH, salinity, and specific ultraviolet absorbance (SUVA). DOM contained hydrophobic compounds and metal ions which can form DOM-PFASs complexes to provide

more sorption sites for PFASs. The finding is useful for executing PFASs remediation by biochar filtration column, especially legacy long chain PFASs, for groundwater remediation.

Keywords

AFFF, PFASs, biochar, sorption, groundwater, DOM

1. Introduction

Aqueous film-forming foams (AFFF) are surfactant products comprising of per- and polyfluoroalkyl substances (PFASs). They are used for extinguishing flammable liquid fuel fires in training and fire-fighting activities at airports and military bases. PFASs seep into groundwater through the soil layer and then in some cases entering the drinking water reservoirs (Baduel et al., 2017; Zhang et al., 2019c). A variety of PFASs has been detected in AFFF-impacted groundwater throughout the world (Dauchy et al., 2019; Sammut et al., 2019; Xu et al., 2021). The concentration of perfluoroalkyl carboxylates (PFCAs) and perfluoroalkyl sulfonates (PFSAs) in groundwater near the firefighting training grounds has been found several orders of magnitude above the drinking water standard of Australia (0.08 μg/L) (Bräunig et al., 2017; Sevices, 2016). Exposure to the AFFF-impacted groundwater, has led to the accumulation of certain types of PFASs within humans. Recent reports have linked PFASs with thyroid hormone disruption, low activity sperm, diabetes and cancer, especially in the blood serum of firefighters and local people who are frequently or acutely exposed to PFASs (Barton et al., 2020; Donat-Vargas et al., 2019a; Donat-Vargas et al., 2019b; Lin et al., 2019; Rotander et al., 2015).

A sustainable method is needed for removing PFASs from groundwater. Anion-exchange resins, polymers and a range of synthetic materials are widely used for the removal of pollutants by adsorption, however they are costly and not a viable solution for developing countries (Lu

et al., 2020). Biochar is a sustainable carbonaceous sorbent that can be produced locally using agriculture and timber waste, compared to traditional activated carbons which are generally produced from fossil fuels (Sørmo et al., 2021). Biochar exhibits comparable PFASs sorption to traditional activated carbon sorbents, and offers substantial benefits such as sustainable values and being an environmentally-friendly alternative (Silvani et al., 2019; Zhang et al., 2019b). Biochar has been applied for a wide range of environmental applications such as groundwater and soil remediation (e.g., pesticide, heavy metals) and amendment (Singh et al., 2014; Xiao et al., 2017). An agriculture waste-based biochar has been chosen to investigate the sorption of PFASs in AFFF-impacted groundwater.

PFASs co-exist in groundwater with other contaminants. The behavior and mechanism of PFASs sorption mainly rely on the characteristics of sorbent, the properties of PFASs, and the matrices of groundwater. Perfluoroalkyl acids (PFAAs) comprise of PFSAs and PFCAs and are commonly detected in groundwater (Bräunig et al., 2017; Yong et al., 2021). Studies that cover mechanistic sorption of PFAAs in groundwater are still lacking and the differences of PFCAs and PFSAs in terms of sorption onto biochar sorbents have not been adequately documented (Park et al., 2020; Sørmo et al., 2021). The effect of functional groups and carbon chain length on the sorption of PFASs to biochar needs further elaboration, particularly in the context of groundwater matrices.

Some studies that have reported PFASs sorption in groundwater covered sorption to different biochars and a semi pilot test of the process of remediating groundwater by biochar (Kundu et al., 2021; Xiao et al., 2017). However, a study of real-world PFASs-impacted groundwater is lacking because actual groundwater contains several co-contaminants which may influence the effectiveness of the process such as pH, salinity, specific ultraviolet absorbance (SUVA) and dissolved organic matter (DOM). These factors are inter-related, co-exist in groundwater and affect PFASs sorption together in a complex way. For instance, the change of pH in

groundwater partly depends on the deprotonation of organic matter surface charge and ions (i.e., Ca^{2+}, Na^{+}). Most of the published studies investigated the effects of those factors without considering their co-presence in groundwater but using PFASs-spiked MQ water with either pH, salinity, synthetic DOM (i.e., fulvic and humic) and DOM-free solutions (Gagliano et al., 2020; Jeon et al., 2011; Nguyen et al., 2020; Yu et al., 2012).

Whether salinity influences PFASs sorption onto carbonaceous materials remains a topic of controversy, potentially due to the complexity of groundwater matrices (Dontsova and Bigham, 2005; Du et al., 2015; Wu et al., 2020). The molecular structure of hydrophobic DOM is similar to that of PFASs to a certain extent, due to the net negative charge and molecular weight (200 – 1,000 Da) (Kothawala et al., 2017). The aromatic DOM contains a hydrophobic backbone like PFASs. These features result in two contradictory influences of DOM on PFASs: competition with PFASs for sorbent sites and providing additional PFAS binding sites on their own (Kothawala et al., 2017; McCleaf et al., 2017; Wu et al., 2020; Yu et al., 2012). The competition or mutual support of DOM for PFASs sorption strongly depends on the concentration and composition of DOM in groundwater (i.e. hydrophobicity). Groundwater may consist of various organic compounds such as hydrophilic acids, proteins, phenolic groups, amino acids and Fe/Al oxides. DOM is able to form complexes with PFASs either by electrostatic interaction or cation bridging with multivalent ions such as Ca^{2+}, Fe^{3+} and Al^{3+} (Gagliano et al., 2020). Overall, these factors (i.e., pH, salinity, SUVA and DOM) have posed challenges in interpreting the effects of groundwater chemistry on PFASs sorption. It is necessary to understand the effects of PFASs properties and groundwater chemistry on PFASs sorption to assess the biochar column for practical application.

Therefore, this work aims to investigate the effects of PFASs properties and groundwater chemistry on PFASs sorption in a rapid small-scale column testing (RSSCT) biochar column. The specific objectives were to (i) determine the influences of PFASs functional groups and

carbon chain length of PFCAs and PFSAs, and (ii) study the synergistic/competitive effects of pH, salinity, SUVA and DOM from different AFFF-impacted groundwater sources on PFASs sorption. This study provides important insight into the sorption of PFASs in a biochar column. The sorption behaviour of PFSAs and PFCAs subgroups in a sophisticated groundwater matrix were explained in detail.

2. Materials and methods

2.1 Standards and reagents

A total of 19 PFAAs were studied, including 11 PFCAs (C_3-C_{13}) and 8 PFSAs (C_4-C_{12}) (Table S1). For quantification, 17 isotopically labelled PFAS standards were used (Table S1). Five other isotopically labelled PFAS standards including $13C_3$-PFHxS, $13C_8$-PFOA, $13C_3$-PFBA, $13C_5$-PFPeA, and $13C_8$-PFOS were spiked for instrument recovery calculations. All PFAAs (≥98% purity) and labelled standards (≥99% purity) were purchased from Wellington Laboratories (Ontario, Canada). All the used chemicals were purchased from Sigma-Aldrich of suitable analytical grade and high purity.

2.2 Sorbents and groundwater

The biochar was derived from agriculture-related waste and used for the PFASs sorption study. The biochar was synthesized from sugarcane bagasse. Sugarcane biochar was chosen for the column study based on the sorption results of the preliminary batch experiment (data not shown). The raw material was dried at room temperature and cut into small pieces (1 - 2 cm), washed by distilled water to phase out contaminants, and dried overnight at 55 ^{o}C. Next, the material was modified to increase the surface area and pore volume. 10 g of the material was incubated in 1 L $MgCl_2$ solution (20 % v/v) by shaking at 120 rpm for 24 h. The mixture was heated at 80 ^{o}C to evaporate the liquid phase. The solid phase was subsequently collected, washed by distilled water and dried at 105 ^{o}C over a 6 h period. Finally, the materials were

pyrolyzed at 550 ºC for 1 h under N_2 gas. The final product was ground, homogenized, and sieved to achieve the effective size (0.5 mm). It was stored in sterile conditions prior to use for this study's experiments.

This study experimented with both PFASs-spiked MQ and AFFF-impacted groundwater. In practice, concentrations of PFASs in the groundwater of Australia can be highly variable ranging from below the limit of detection to 100 µg/L (Phong Vo et al., 2020). The initial concentration of each PFASs in PFASs-spiked MQ was chosen at 10 µg/L. Some groundwater sources possessed long chain PFASs up to C_{14} (Wei et al., 2018), but most of them did not because long chain PFASs were retained by the soil (Bräunig et al., 2017; Murray et al., 2019; Yong et al., 2021). The short chain and long chain PFASs have been defined previously (Buck et al., 2011). The short chain PFCAs and PFSAs have less than six and five perfluorinated carbons, respectively; and vice versa for the long chain PFCAs and PFSAs.

We prepared the PFASs-spiked MQ having carbon chain length up to C_{13} for two reasons. The first one is to calculate the log partitioning coefficient (log K_d) of PFCAs and PFSAs in the ideal condition. Then, the log K_d results are used to validate the effect of groundwater chemistry on PFASs sorption. The groundwater samples were collected at four different bores (i.e., B1, B2, B3 and B4) near the firefighting training ground in Queensland (Australia) (Table 1).

Table 1. Concentration of PFASs (µg/L) and other key parameters in four AFFF-impacted groundwaters (n=2). Numbers in brackets are standard deviation (SD)

	B1	B2	B3	B4
PFBA (C3)	2.4 (0.06)	< LOD	< LOD	< LOD
PFPeA (C4)	4.4 (0.45)	< LOD	< LOD	< LOD
PFHxA (C5)	11.1 (0.05)	< LOD	< LOD	1 (0.01)
PFHpA (C6)	3.3 (0.2)	< LOD	< LOD	< LOD
PFOA (C7)	6.1 (0.22)	0.3 (0.002)	< LOD	0.2 (0.01)

PFNA (C8)	0.4 (0.02)	0.5 (0.003)	< LOD	< LOD
PFDA (C9)	< LOD	0.4 (0.03)	< LOD	< LOD
PFUnDA (C10)	< LOD	< LOD	< LOD	< LOD
PFDoDA (C11)	< LOD	< LOD	< LOD	< LOD
PFTriDA (C12)	< LOD	< LOD	< LOD	< LOD
PFTeDA (C13)	< LOD	< LOD	< LOD	< LOD
PFHxDA (C15)	< LOD	< LOD	< LOD	< LOD
PFODA (C17)	< LOD	< LOD	< LOD	< LOD
PFBS (C4)	2.9 (0.08)	< LOD	< LOD	0.6 (0.01)
PFPeS (C5)	2.6 (0.1)	< LOD	< LOD	0.6 (0.03)
PFHxS (C6)	22.2 (1.2)	0.26 (0.02)	0.7 (0.05)	5.5 (0.2)
PFHpS (C7)	2.4 (0.08)	< LOD	< LOD	0.2 (0.02)
PFOS (C8)	72.1 (0.01)	2.1 (0.03)	0.8 (0.04)	2.8 (0.13)
PFNS (C9)	< LOD	< LOD	< LOD	< LOD
PFDS (C10)	< LOD	< LOD	< LOD	< LOD
PFDoDS (C12)	< LOD	< LOD	< LOD	< LOD
pH	7.8	7.6	7.1	7.1
Salinity (%)	0.26	0.02	0.02	0.22
DOM (mg/L)	4.6 (0.1)	6.5 (0.1)	6.6 (0.1)	10.9 (0.2)
SUVA (L/mg.m)	8.3 (0.1)	4.8 (0.1)	4.8 (0.1)	0.8 (0.1)

*Limit of detection (LOD) = 0.1 µg/L

2.3 Column sorption study

We conducted a PFASs sorption analysis using the biochar-based RSSCT experiments. RSSCT is an alternative method which is based on the simulation of a full-scale column. RSSCT is a scaled-down version of the full-scale system and has been applied successfully to predict the breakthrough profiles of PFASs (McCleaf et al., 2017; Park et al., 2020). The RSSCT was designed following the suggestion of previous studies (McCleaf et al., 2017; Park et al., 2020). A syringe (5 ml) was filled with 500 mg sugarcane biochar. The syringe type was selected to eliminate the channelling effects because the ratio of column diameter to particle diameter was greater than 50 (Park et al., 2020). The biochar bed was compressed by a piston until it was sufficiently tight enough to create a packed bed of 2.25 cm in height. Five identical columns were created for five groundwaters. Characteristics of the groundwater are summarized in

Table 2. The column was activated by MQ water which functioned to remove air in the media bed, keep it water-saturated and release the potential DOM and alkalinity presented in biochar (Smebye et al., 2016). A low flow rate of 0.5 ml/min was set to suppress any dispersion effect. The Reynolds number at this flowrate was 0.05. The linear velocity in the column is 0.438 cm/min.

The concentrations of sorbates in the column effluent were used to develop the breakthrough profiles of PFASs as a function of eluted bed volumes. The value of 1 bed volume (BV) was approximately 2.0 mL. Fractions were collected every 20 min into 15 ml polypropylene tubes. The total experiment time was 8 h. Before sampling, all the tubes were centrifuged at 3,000 rpm for 20 min at 20 ^{o}C, 250 μL of each sample was collected into microcentrifugation tubes and then further centrifuged at 14,000 rpm for 20 min at 20 ^{o}C to eliminate residual biochar. The final solute (200 μL) was transferred to a vial containing 200 μL methanol (99.8%, LiChrosolv®, Sigma-Aldrich). The mass-labelled and recovery internal standards were spiked at 4 ng/ml prior to performing LC-MS analysis.

2.4 Surface area, pore volume, salinity and dissolved organic matter and specific UVA analysis

The surface area and pore volume of the sorbents were determined using Brunauer-Emmett-Teller (BET) analyzer (Quantachrome Autosorb IQ, USA) with the sorption/desorption isotherm of nitrogen at 77 K. Firstly, degassing of the sorbents was carried out in vacuum conditions at 473 K and lasted 6 h. Surface area and pore size distribution were calculated via the Density Functional Theory algorithm. The pore size in the sorbent is divided into three groups: micropore (< 2 nm), mesopore (2 – 50 nm) and macropore (>50 nm). This sorbent comprises macropore and mesopore only (Table 2).

177 Table 2. Surface area and pore volume distribution of the $MgCl_2$ modified sugarcane biochar.
178 Numbers in brackets are standard deviation (SD).

Pore size	Surface area distribution (m^2/g)	Pore volume distribution (mm^3/g)
Micropore (<2 nm)	81.3 (0.15)-	76.25 (4)
Mesopore (2 – 50 nm)	14.8 (0.1)	45.81 (5)
Macropore (>50 nm)	-	-

179 The salinity of groundwater was measured using a salt meter (Horiba, Japan). Concentrations
180 of DOM were analysed by Multi N/C 3100 (Analytik Jena, Germany). The groundwater
181 samples were pre-filtered before analysis using 0.45 μm syringe filters (Phenex™-GF 28 mm)
182 to eliminate the particulate organic matter. In this study, we assumed that DOM was equivalent
183 to dissolved organic carbon (DOC) due to the negligible amount of dissolved organic nitrogen
184 and other compounds in the groundwater (5 – 7%) (Connolly et al., 2020). The SUVA was
185 calculated from Eq. 1 below.

186 $$\text{SUVA} = \frac{UV_{254}}{DOC} \times 100 \quad \text{(Eq. 1)}$$

187 Where SUVA is specific UVA (L/mg.m), UV_{254} is UV absorbance at 254 nm (1/cm) and DOC
188 is dissolved organic carbon (mg/L).

189 2.5 Partitioning coefficient of PFASs onto biochar in the column

190 The partitioning coefficient (K_d) was estimated by using breakthrough column
191 chromatographic data. This was achieved by keeping the volumetric flowrate and the carrier
192 flowrate constant. This was possible since the concentration of adsorbed species was
193 significantly small. The PFASs concentration in the pores is assumed to equal to the bulk
194 groundwater concentration. In detail, the partitioning coefficient was calculated by the mass
195 balance equation (Eq. 2) below:

196 $$\left[\varepsilon_b + (1-\varepsilon_b)\left(\varepsilon_p + \left(1-\varepsilon_p\right)K_d\rho_s\right)\right]V = F\int_0^\infty \frac{(C_0-C)}{C}dt$$

197 (Eq.2)

198 Where K_d (L/kg) is the partitioning coefficient, V is the column volume, F is the volumetric
199 flowrate, C is the equilibrium or near-equilibrium concentration (at 8h), C_0 is the feed
200 concentration, ε is the porosity (b for bed and p for particle) and ρ_s is the density of sorbent.

201 2.6 Quantitative LC-MS/MS analysis

202 The PFASs analysis method was described recently elsewhere (Bräunig et al., 2019; Nguyen
203 et al., 2020). PFASs were analysed using high performance liquid chromatography (Nexera
204 HPLC, Shimadzu Corp., Japan) coupled to a tandem mass spectrometer (QTrap 5500 AB-
205 Sciex, Ontario, Canada). The polar C18 Luna Omega column (100 x 2.1 mm) had a particle
206 size 1.6 µm, and pore size of 100 Å. The mobile phases consist of A phase of 10 mM
207 ammonium acetate in Milli-Q water, acetonitrile and acetic acid (94.9:5:0.1, v/v), and B phase
208 of 0.5 mM ammonium acetate in acetonitrile, Milli-Q water and acetic acid (94.9:5:0.1, v/v).
209 The negative electrospray ionization mode was employed. The injection volume was 10 µL
210 holding at a temperature of 50 ºC. A pretreatment column (C18, 50 × 4.6 mm, 5 µm,
211 Phenomenex, Lane Cove, Australia) was set up between the solvent and injector to delay
212 PFASs background. PFASs quantification was calculated by mass-labelled internal standard.
213 An eight-point calibration standard was prepared with concentrations ranging from 0.1 to 100
214 µg/L.

215 For quantitative analysis, the calibration standards were weighted linearly through 1/x
216 regression. The requirement for regression coefficients was ≥ 0.993. Analytical replications
217 were performed once in every five injections together with two points of the calibration
218 standards being reanalysed after 10 samples. The full calibration standards were analysed both
219 at the beginning and the end of each analytical batch. A maximum variation of 10% among

analytical replications was considered acceptable. Procedural blanks and samples spiked with a known amount of PFASs were also performed in duplicate. The limits of detection (LODs), and limits of quantification (LOQs) were reported elsewhere (Nguyen et al., 2020).

2.7 Principal component analysis

Origin Pro 2017 (Origin Lab) was used to perform principal component analysis (PCA) analysis and evaluate the correlation of partitioning coefficients K_d of PFCAs/PFSAs and selected groundwater chemistry factors (i.e., pH, salinity, SUVA and DOM). The dataset for PCA analysis is summarized in Table S5.

3. Results and discussion

3.1 Partitioning coefficients of PFASs onto biochar in PFAS-spiked MQ water and AFFF-impacted groundwater

To elaborate on the sorption behaviour of PFASs, partitioning coefficients (presented as log K_d) of PFASs between biochar and the aqueous phase were calculated (Fig. 1). Generally, the PFSAs demonstrated higher log K_d than PFCAs given a similar perfluorinated carbon chain length. For example, in the PFASs-spiked MQ samples, log K_d of PFOS was 1.57 log units which were 1.3 times higher than the log K_d of PFNA (1.18 log units). Also, the long chain PFASs exhibited better partitioning on the sorbent compared to short chain PFASs. There is a trend of increasing log K_d with the increasing numbers of perfluorinated carbons. Log K_d of long chain PFASs ranged from 0.77 to 4.63 log units, while for short chain PFASs, log K_d stayed below 0.68 log units. The trends were consistent for both PFASs-spiked MQ and AFFF-impacted groundwater and agreed with previous studies (Oliver et al., 2020; Xiao et al., 2017; Zhang et al., 2019a). Further discussion on the influence of functional groups and carbon chain length on PFASs sorption is provided in section 3.2.

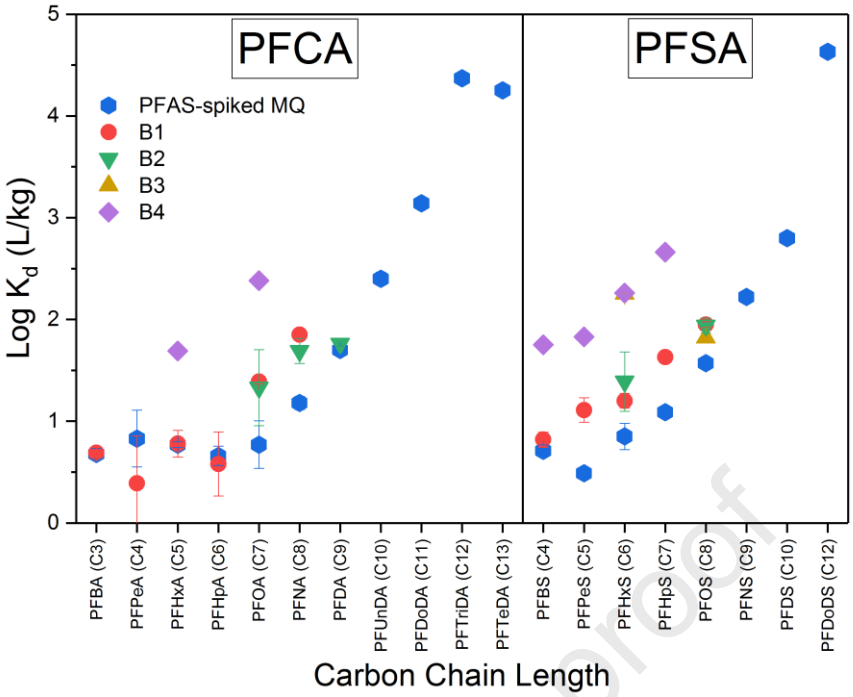

Fig. 1. Log K_d for sorption of PFCAs and PFSAs in PFAS-spiked MQ water and AFFF-impacted groundwater onto biochar. PFASs in each groundwater type were examined in distinct colors and symbols. All measures show significant differences ($p<0.01$). The K_d values of the PFASs-spiked MQ and AFFF-impacted groundwater are given in detail in Table S4. All measures showed significant differences ($p < 0.05$) amongst log K_d of groundwater sources.

3.2 Effects of PFASs properties

3.2.1 Functional groups

The functional groups consist of the carboxylic group for PFCAs and the sulfonic group for PFSAs. The PFSAs possessed higher log K_d values than PFCAs given a similar number of perfluorinated carbons (Fig. 1 and Table S4). From Fig. 2, it shows a linear correlation of log K_d and retention time of PFASs in the LC-MS column (Adjusted R^2 = 0.79 – 0.83). The retention time of PFAS in the LC-MS column is a typical proxy indicating the hydrophobicity of PFASs (Xiao et al., 2017). The slope of PFCAs linear fit was 1.18 which was slightly less than the value of PFCAs, being 1.45. It indicated that PFSAs were retained much more than PFCAs; in fact, it was 1.3-fold due to the higher hydrophobicity. The smaller size of the

carboxylic functional group of PFCAs possibly made it less hydrophobic than the sulfonic functional group (Oliver et al., 2020). Recently, Wang et al. (2019) stated that PFSAs exhibited higher sorption affinity than PFCAs. Park et al. (2020) established the correlation between half-breakthrough bed volume (BV_{50}) and octanol-water partition coefficient (log D_{ow}) of PFASs to predict the sorption behaviour, but it was monotonic and did not reflect the discrepancy of PFCAs and PFSAs that we found. Higgins and Luthy (2006) reported that PFSAs showed 1.7-fold higher hydrophobicity than PFCAs which was slightly higher than our value. This is probably attributed to the discrepancies of soil and groundwater matrices, and properties of sorbents and feedstocks used for producing the biochar. For instance, the surface area of pinewood biochar of 351 m^2/g was 4 times higher than the sugarcane biochar of this study (Xiao et al., 2017). The pinewood biochar of Xiao et al. (2017) was prepared by gasification method, which differs from the pyrolysis method of this study. The other types of biochar prepared by pyrolysis method showed less surface area than our biochar. Higher surface area could provide more binding sites for PFAS even other larger sorbates such as DOM could block the micropore (Ando et al., 2010; Wu et al., 2020). The finding indicates the characteristics of biochar which defines the PFAS sorption efficiency also depends on the methods used to produced biochar (Muvhiiwa et al., 2019).

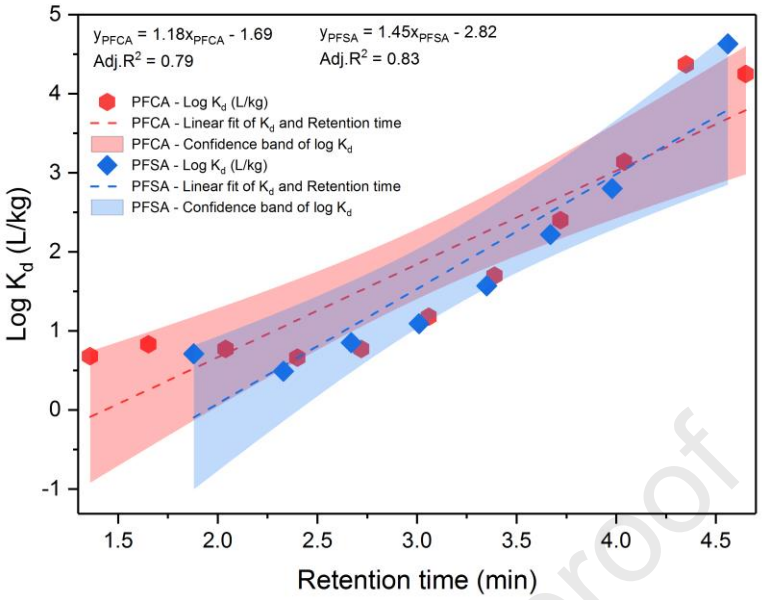

Fig. 2. Correlation of PFASs retention time in the LC-MS column and log K_d of PFCAs and PFSAs groups. The details of PFASs retention time in a LC-MS column can be found in Table S5. The log K_d values were obtained from PFAS-spiked MQ water.

3.2.2 Carbon chain length

The longer chain PFASs of the same group showed higher log K_d values resulting from the extensive dominance of long chain PFASs on sorbent sites and pores over short chain PFASs (Xiao et al., 2017). The increase of log K_d per CF_2 moiety also differs between the short chain and long chain PFASs. For short chain PFASs, the increasing trend of log K_d per CF_2 moiety is not clearly observed which is potentially due to the low sorption efficiency and hydrophobicity of short chain PFASs. For long chain PFASs, log K_d increases 0.5 and 0.8 for each CF_2 moiety of PFCAs and PFSAs respectively. It is caused by the increase of hydrophobicity of long chain PFASs proportional to the amount of perfluorinated carbons, which refers to the rule of additivity (Park et al., 2020). The observation of increasing log K_d overall agrees with other studies, but log K_d values are sorbent specific (Park et al., 2020; Xiao et al., 2017). Some sorbents exhibit higher sorption affinity with more porosity. For instance,

commercial activated carbon (F300) achieved 4 to 5.5 log K_d for short chain PFASs which is much higher than the biochar from this study (Xiao et al., 2017). However, the flow patterns of sorption experiment also pose certain influence on the value of log K_d. Although the K_d calculation of this study primes by the equilibrium sorption, the K_d values might be underestimated by higher flow rates which would restrain the diffusion of PFAS to the micropore.

The breakthrough profiles of selected PFASs in PFASs-spiked MQ water and AFFF-impacted groundwater are shown in Fig. 4 and Fig. S1. The shorter chain PFASs demonstrated shallower breakthrough curves and smaller BV_{50} values. For example, in the B4 samples, the order of BV_{50} values was PFOS>PFHxS>PFHxA which agreed with the effects of PFASs properties on sorption behavior. The data reported in other studies agreed with what we have found (Dalahmeh et al., 2019; Liu et al., 2019; Park et al., 2020). However, the amount of BV in this study was less than what other researches documented (McCleaf et al., 2017; Park et al., 2020). The threshold of BV in this RSSCT column was 120 while the noted studies reported BV up to 150,000. The operation of RSSCT and BV_{50} depended on various engineering factors such as initial PFASs concentrations, numbers of PFASs, depth of the packed bed, and characteristics of the sorbent (Murray et al., 2019; Xiao et al., 2017). For instance, we experimented with 19 PFASs substances, having an initial concentration of 10 μg/L. Park et al. (2020) and McCleaf et al. (2017) used the initial PFASs concentration ranging from 0.1 to 0.35 μg/L which was less than our values by 30- to 100-fold.

3.3 Effects of groundwater chemistry

3.3.1 Contributions of factors in groundwater to PFASs sorption

The matrix of groundwater is diverse and has a complex effect on the sorption of PFAS to biochar. Groundwater chemistry has been widely recognized as exerting effects on the sorption

316 of the charged organic molecules (Higgins and Luthy, 2006; Park et al., 2020). To evaluate the
317 effects of groundwater chemistry on PFASs sorption, we conducted PCA analysis to describe
318 the relative correlation between K_d of PFCAs/PFSAs groups and the groundwater chemistry
319 factors (i.e., pH, salinity, SUVA and DOM) (Fig. 3).

320 The first factor is pH which ranged from 7.1 to 7.8 in the four groundwater samples. The pKa
321 values of all PFASs in this study were below 2 which meant that the speciation of PFASs was
322 unchanged (Ahrens et al., 2012; Goss, 2008). It means any pH influences observed are
323 attributed to the pH-related changes in the sorbents, such as organic matter charge, and less
324 likely due to protonation/deprotonation of PFASs (Higgins and Luthy, 2006). The salinity
325 posed certain effects on PFASs sorption and was strongly related to the presence of divalent
326 cations in groundwater such as Ca^{2+} and Mg^{2+} (Wu et al., 2020).

327 Monovalent ions did not reveal a particular influence on anionic PFASs sorption but divalent
328 ions did (Higgins and Luthy, 2006). The divalent cations were present at high concentrations
329 in B1 and B4 groundwater samples (i.e., 7 - 419 mg Ca^{2+}/L and 1 - 277 mg Mg^{2+}/L) (Army
330 Aviation Centre Oakey, 2019). The increase in Ca^{2+} enhanced sorption of anionic sorbate onto
331 the sorbent due to the salting out and cation-bridging effects (Dontsova and Bigham, 2005; Du
332 et al., 2015). Salinity itself does not adequately explain the increase of K_d but it should be
333 placed in a joint context with SUVA and DOM. The divalent cations inter-correlated with
334 DOM by influencing the deprotonation of DOM (Jeon et al., 2011). B1, B2 and B3 samples
335 contained high aromaticity (SUVA>2 L/mg.m) whereas B4 possessed lower aromaticity
336 (SUVA<2 L/mg.m). The aromatic substances are hydrophobic which attract PFASs and
337 increase PFASs sorption (Park et al., 2020; Wu et al., 2020). However, our PCA analysis shows
338 that SUVA influences PFASs sorption to a lesser extent than salinity and DOM.

339 The PCA analysis suggests that DOM influences PFASs sorption the most critically in this
340 study. According to Appleman et al. (2013), a DOM concentration of 1.7 mg/L could increase

the breakthrough time of PFASs compared to deionized water. The DOM concentrations of four AFFF-impacted groundwater sources in this study were more than 2 mg/L, indicating a significant impact of DOM on the sorption behaviour of PFASs. In Fig. 1, log K_d values of PFASs in the AFFF-impacted groundwaters exceeded the PFASs-spiked MQ 1 - 1.5 logs. The higher DOM concentration in groundwater samples resulted in higher log K_d values. Kothawala et al. (2017) and McCleaf et al. (2017) agreed with our result that the increase of DOM in water samples facilitates PFASs sorption. McCleaf et al. (2017) has found that after operating the column for 50d, the removal efficiency of PFAS increased which might be attributed to the loading of DOM on sorbent and agglomeration of PFAS. Some studies reported different findings that DOM did not affect PFAS sorption or could reduce it (Wu et al., 2020; Yu et al., 2012). For instance, Wu et al. (2020) performed a PCA analysis and concluded that DOM did not perform inhibition to PFAS sorption. However, the analysis of Wu et al. (2020) used the data of both positive charged (β-cyclodextrin polymers) and negative charged (activated carbons) sorbents. Wu et al. (2020) also indicated that DOM may only influence PFAS sorption on negative charged sorbent like our case. Yu et al. (2012) investigated that DOM impaired the PFAS sorption from 15% to 30% due to the pore blockage and competition of sorbent sites by DOM. The degree of DOM effect depended on the molecular size distribution of DOM. DOM having size larger than 30 kDa showed similar sorption efficiency to DOM-free solution; in turn, low molecular weight DOM (<1 kDa) demonstrated greater effect. It implied that the effect of DOM on PFAS sorption was also subjected to the specific characteristic of groundwater. In addition, Yu et al. (2012) used the DOM-spiked artificial groundwater which ignored other matrices, while our study, Kothawala et al. (2017) and McCleaf et al. (2017) experimented with the real surface and groundwater. The potential reason for the disparity of those studies is the pollutants transport patterns of sorption studies (i.e., batch and column, flow rate) which undermine the influence of DOM. Another important underlying reason is that

366 multivalent cations presented in real groundwater can form DOM-PFASs complexes which
367 retain much more PFASs in the column (section 3.3.2).

368 This PCA analysis includes 6 variables and 4 observations which are similar to Wu et al. (2020)
369 consisting of 7 variables and 12 observations (i.e., 3 sorbents in 4 groundwater sources). This
370 study focuses on only one type of sorbent so the number of observations is less than Wu et al.
371 (2020), which is a limit that needs to be addressed in the future.

372

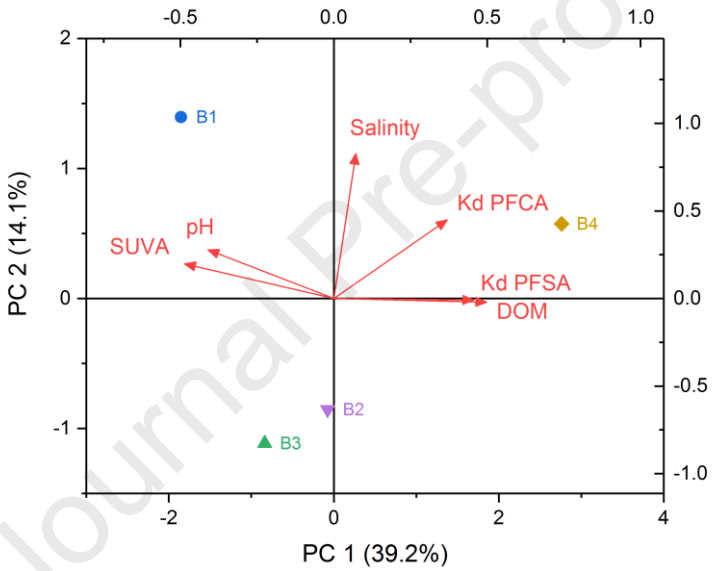

373

374 Fig. 3. PCA biplot showing the correlations of the groundwater chemistry and the partitioning coefficients per
375 CF_2 moiety of PFCAs and PFSAs (calculated by Eq. S1 and Eq. S2). The PCA was created by the multi-
376 dimensional dataset with 6 variables and 4 observations. The variables are plotted by the straight arrows.
377 Correlations between the variables are shown through the angles in between the two arrows. The observations
378 were plotted as points in different colors and symbols. The degrees of observations for the variables are
379 demonstrated via the relative distance of the points to the arrows.

380 3.3.2 How DOM influence PFASs sorption?

381 The effects of DOM on the sorption behavior of PFASs are indicated through the breakthrough
382 profiles (Fig. 4). For PFHxA, PFHxS and PFOA, the effect of DOM on the breakthrough

383 profiles was not significantly different (Fig. 4a, b, c). Importantly, the breakthrough profiles of
384 PFOS did not follow the general trend like other PFASs and this requires further elaboration
385 (Fig. 4d). In B4 sample, PFOS reached BV_{50} more slowly and did not reach the point of
386 exhaustion within the studied timeframe. The discrepancy in the PFOS breakthrough profiles
387 was strongly attributed to the variation of DOM levels presented in four groundwater sources.

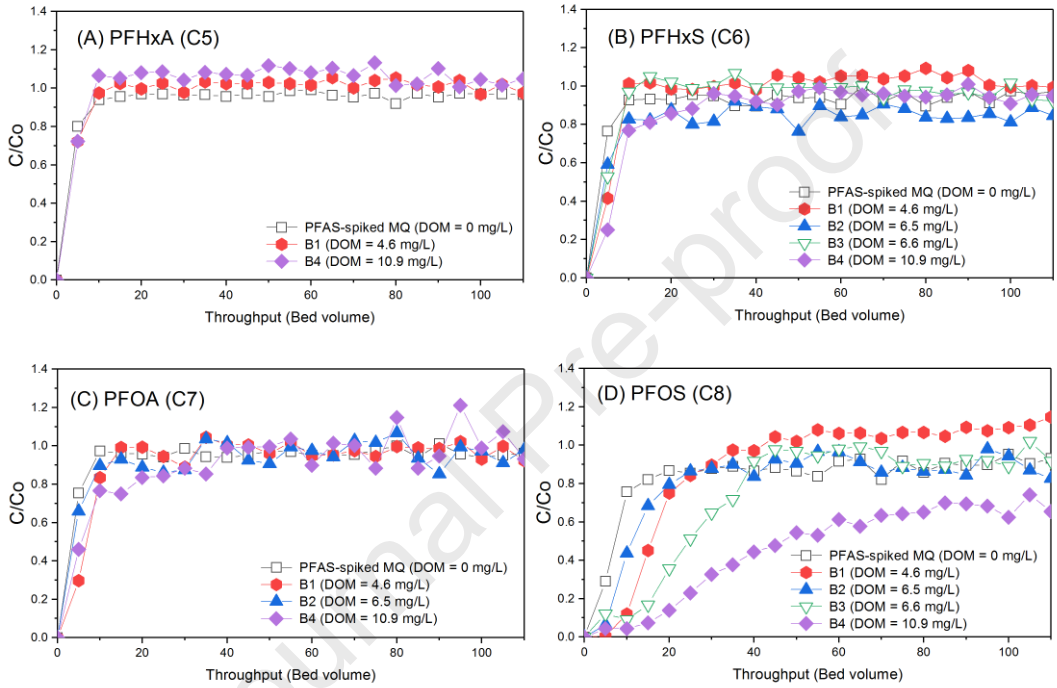

388

389 Fig. 4. Breakthrough profiles of selected PFASs in the AFFF-impacted groundwater sources: PFHxA (panel A),
390 PFHxS (panel B), PFOA (panel C), and PFOS (panel D). The PFASs collected in the similar location are denoted
391 with an identical symbol and color pattern. Concentrations of the selected PFASs in the panels are beyond the
392 detection limit (>0.1 µg/L).

393 DOM demonstrated a significant influence on the breakthrough behavior of PFASs showed
394 through the correlation of BV_{50} and DOM concentrations (Appleman et al., 2013; McCleaf et
395 al., 2017). The BV_{50} was selected for establishing the correlation with DOM because it
396 reflected the apparent PFASs sorption capacity of biochar (Corwin and Summers, 2011).
397 Interestingly, we found that the concentration of DOM correlated significantly to BV_{50} of PFOS

(Fig. 5a) (R^2=0.68). This was despite the difference in the initial concentration of PFASs and other types of interference, for example pH. This correlation has confirmed the significant effect of DOM on sorption of PFASs in groundwater, rather than pH, at least in the scope of this research.

The composition of DOM also played an important role in the sorption of PFASs. This phenomenon has not been fully explained in previous studies. With UV scanning, we discovered that groundwater samples contained large amounts of hydrophobic DOM (Fig. 5b). The Bz band (190-240 nm) presented the aromatic compounds based on the transition and vibration perturbation of the Π-e system (Korshin et al., 1997). The absorbances of all samples are higher than 0.5, possibly containing hydrophobic DOM which can form DOM-PFASs complexes and increase PFAS sorption. The ET band (240–400 nm) exhibited hydrophilic functional groups such as hydroxyl, carboxyl, carbonyl and ester varieties. The absorbances of the hydrophilic regions are all lower than 0.5, thus demonstrating the minor hydrophilic DOM fraction of the groundwater samples.

DOM competes with PFASs and occupies the sorption sites within the pores of the sorbent. At neutral pH, DOM was deprotonated so that it was negatively charged creating electrostatic repulsion between the negatively charged functional group of PFASs (Choppin and Kullberg, 1978). The short chain PFASs were subject to electrostatic repulsion and consequently absorbed less than the long chain PFASs. However, DOM could provide more sorption sites for PFASs on their own surfaces. Those DOM were hydrophobic which meant they were able to entrap hydrophobic PFASs and form DOM-PFASs complexes on the uncharged sites. DOM can also create cation bridging with multivalent ions such as Fe^{3+} and Al^{3+} (Gagliano et al., 2020). For example, the carboxyl group of PFOA could create a complex structure with Fe and Al oxide in groundwater (Xiao et al., 2019). DOM is present in groundwater in much higher concentrations than PFASs and therefore retained PFASs extensively, proportional to the

423 increase of DOM. This was the solid-phase dissolution process and the main reason for the
424 increase of K_d values in higher DOM concentrations. In this study, we exclude the possibility
425 of DOM desorption in the eluent because biochar was washed and activated with MQ water.
426 Previous work has shown that washing reduced alkalinity of biochar leading to the reduction
427 of final pH in the mixture of biochar and groundwater (Smebye et al., 2016). In addition, the
428 biochar of this study was modified with $MgCl_2$ to have positive charge sites for sorption of
429 DOM and PFASs, even at high pH (Fang et al., 2020). Hence, the effect of DOM desorption
430 on the result is not apparent.

431 To further verify this assertion, sorbent was collected at the top and middle of the RSSCT
432 media bed and processed through FTIR (Fig. 5c, d). The spectra of 1390 cm^{-1} in both
433 groundwater samples indicated the presence of monodentate which is a complex of iron
434 structure and the PFASs carboxyl group. On the FTIR spectra, several bands could be observed,
435 indicating the sorption of PFASs and organic matter on sorbents. Bands observed at 2992 cm^{-1}
436 and 3672 cm^{-1} depicted C-H and O-H stretches of aromatic and phenol substances,
437 respectively. Those bands coincided with the data produced by UV scanning and confirmed
438 the competitive sorption of PFASs and hydrophobic organic matter in groundwater samples.
439 Likewise, the bands of 1078 cm^{-1}, 1250 cm^{-1}, 1580 cm^{-1} and 873 cm^{-1} represent sulfonic group,
440 C-F stretching, C=O stretching of carboxylic group and absorbance of CF_2 and CF_3,
441 respectively (Guo et al., 2017).

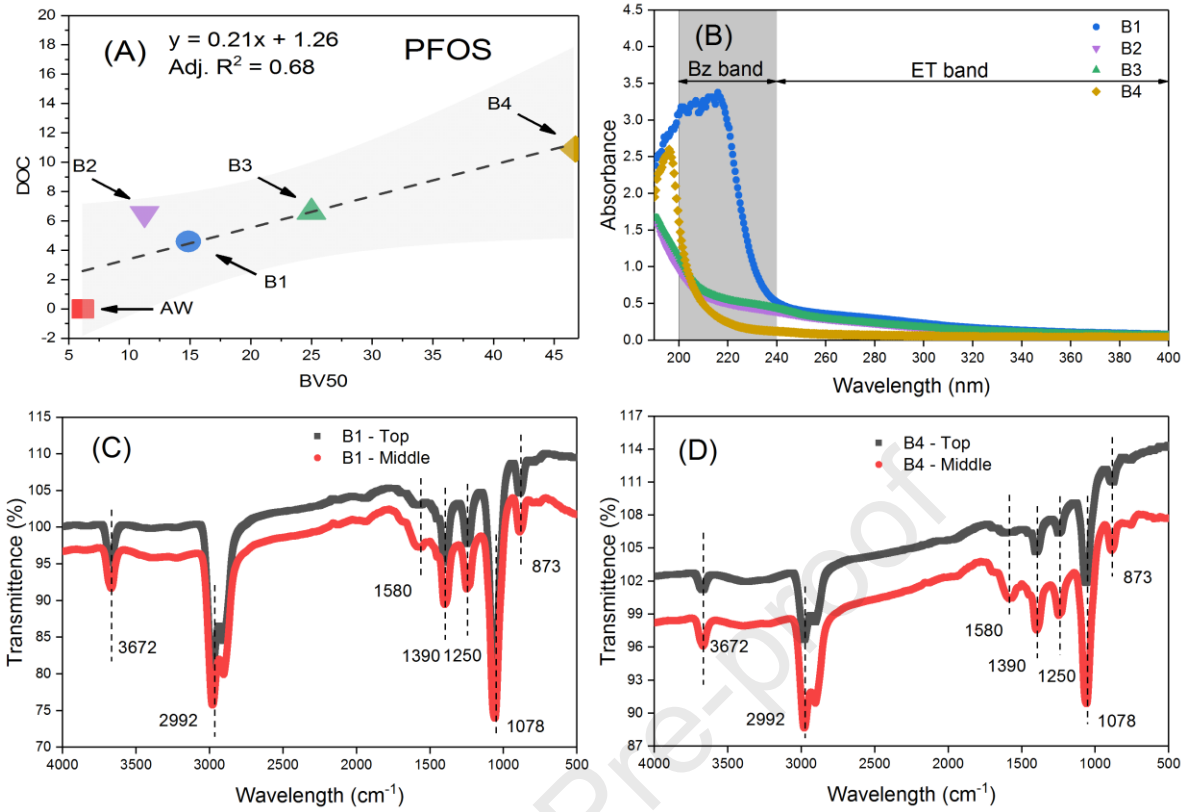

Fig. 5. Correlation of DOM in groundwater samples and BV_{50} of PFOS in RSSCT (panel A), UV scan profiles of groundwater samples (panel B), FTIR scan of sorbent on top and middle of RSSCT media bed of the B1 sample (panel C) and B4 sample (panel D). The dashed line and shaded area in panel A show linear fit and 95% confidence band, respectively. The y axis presents the DOM concentration (panel A), absorbance (panel B) and transmittance (panel C, D).

3.4 Environmental implications

The finding of this study is subjected to only one biochar (sugarcane bagasse pyrolyzed at 550 ^{o}C). In essence, future studies need to investigate the effect of biochar produced from various feedstocks (e.g., corn straw, timber, biosolid) and processes (e.g., pyrolyzed temperature and pretreatment methods). For example, corn straw-derived biochar showed higher PFAS sorption efficiency at higher pyrolysis temperatures (700 ^{o}C and 550 ^{o}C)(Guo et al., 2017). The higher pyrolysis temperature could increase surface area and pore volume of biochar up to 10-fold (Guo et al., 2017). At 500 ^{o}C, pyrolysis can be combined with biochar pretreatment by chemical activation, such as $ZnCl_2$ and H_2SO_4, to increase microporosity (Martin et al., 1996). Those

457 experiments, together with this study, will provide adequately the sorption capacity of biochar
458 and relevant mechanisms of PFAS sorption.

459 The data presented demonstrate a potential control alternative to alleviate the risk for
460 communities who are exposed to PFASs-impacted groundwater. It provides an insight into the
461 understanding and applicability of PFASs sorption by biochar which could be used for
462 upscaling and field deployment. The removal of long chain PFASs by biochar is viable. The
463 application can be further extended for sorption of emerging PFASs such as other anionic,
464 nonionic and zwitterionic variations whose toxicity and bioaccumulation potential in AFFF-
465 impacted groundwater are not fully investigated. Further validating research is also required.
466 Although other sorbents (i.e., ion exchange resin, β-cyclodextrin, Rembind®) and technologies
467 (membrane, advanced oxidation process) might be more effective in PFASs remediation,
468 biochar is more beneficial in cost and sustainable values (Phong Vo et al., 2020). For instance,
469 the commercial price of biochar is $246 – 500/tonne which was 3-5 times less than activated
470 carbon ($1500 US/tonne) (Ahmad et al., 2014; Mohan et al., 2014). Sørmo et al. (2021) applied
471 5% biochar dose to immobilize PFASs leaching from the soil, while Hale et al. (2017) did for
472 3% activated carbon. In practice, the applied dose of biochar depended on several factors (e.g.,
473 sorbent characteristic and water matrix) which would decide the ultimate cost of using biochar
474 for PFAS remediation. Apart from soil immobilization, biochar can also be reused in thermal
475 treatment. The addition of activated biochar significantly enhances the sorption of gas-phase
476 PFAS on biochar and increases PFAS decomposition (Sasi et al., 2021). The application of this
477 biochar depends on the availability of raw material, environmental protection strategy of local
478 government and expectation of end-users. This sugarcane bagasse biochar is potential for
479 regions where sugarcane is the main agricultural product.

480 Effects of groundwater matrix, particularly DOM, is an important point to look at before
481 designing field scale works. This study provides mechanistic interaction of DOM and PFASs

in various groundwater matrices. Some of the breakthrough profiles are however near-equilibrium conditions which needs further elaboration as, in practice, the near one is not expected to happen. Batch experiments do not completely show the effect of DOM on the sorption of pollutants due to different pollutants transport pattern. For instance, flow rate in the column is an important factor determining the diffusion of pollutants into micropore. It is challenging to use the results of batch conditions for upscaling, but the result of a column study could work (Kothawala et al., 2017). This would be a motivation for future studies to uncover the effects of groundwater matrix to PFASs sorption. In addition, attention to the engineering factors of the column such as sorbent bed depth, hydraulic retention time, recirculation potential and sorbent regeneration is required.

4. Conclusions

This study investigates the effects of PFASs properties and groundwater chemistry on PFASs sorption in a biochar column. By using PFAS-spiked MQ and AFFF-impacted groundwater, the following important conclusions can be made:

- The sorption of PFSAs towards biochar sorbent was 1.3-fold higher than that of PFCAs. Log K_d of long chain PFASs ranged from 0.77 to 4.63 log units while it was below 0.68 log units for short chain PFAS. Log K_d values of PFASs in the real AFFF-impacted groundwater were higher than the PFASs-spiked MQ water 1 - 1.5 log magnitude due to the effect of the groundwater matrix.

- Amongst the selected factors in groundwater (i.e., pH, salinity, SUVA, DOM), DOM had the most significant influence on PFAS sorption determined via PCA analysis. DOM contained hydrophobic compounds and complexes (e.g., monodentate) which could compete with PFASs and also provide sorption sites for PFAS.

Further works are suggested for a field-scale study to fully evaluate the effects of environmental matrix and applicability of biochar for AFFF-impacted water sources.

Acknowledgement

This research was supported by University of Technology Sydney, Australia (UTS, RIA NGO). The authors acknowledge Prof. Jochen F. Mueller and Dr. Jennifer Bräunig for reading the manuscript, providing critical comments and PFASs analysis support.

References

1. AECOM, 2016. Stage 2C Environmental Investigation. Available from: https://www.defence.gov.au/Environment/PFAS/Docs/Oakey/FactSheets/OakeyFactSheetJuly2016.pdf. Accessed 21 May 2021
2. Ahmad, M., Rajapaksha, A.U., Lim, J.E., Zhang, M., Bolan, N., Mohan, D., Vithanage, M., Lee, S.S., Ok, Y.S., 2014. Biochar as a sorbent for contaminant management in soil and water: A review. *Chemosphere*, 99, 19-33.
3. Ahrens, L., Harner, T., Shoeib, M., Lane, D.A., Murphy, J.G., 2012. Improved Characterization of Gas–Particle Partitioning for Per- and Polyfluoroalkyl Substances in the Atmosphere Using Annular Diffusion Denuder Samplers. *Environ. Sci. Technol.*, 46(13), 7199-7206.
4. Ando, N., Matsui, Y., Kurotobi, R., Nakano, Y., Matsushita, T., Ohno, K., 2010. Comparison of natural organic matter adsorption capacities of super-powdered activated carbon and powdered activated Carbon. *Water Res.*, 44(14), 4127-4136.
5. Appleman, T.D., Dickenson, E.R.V., Bellona, C., Higgins, C.P., 2013. Nanofiltration and granular activated carbon treatment of perfluoroalkyl acids. *J. Hazard. Mater.*, 260, 740-746.
6. Army Aviation Centre Oakey, A. 2019. Groundwater and Surface Water Monitoring: April/May 2019.
7. Baduel, C., Mueller, J.F., Rotander, A., Corfield, J., Gomez-Ramos, M.-J., 2017. Discovery of novel per- and polyfluoroalkyl substances (PFASs) at a fire fighting training ground and preliminary investigation of their fate and mobility. *Chemosphere*, 185, 1030-1038.

8. Barton, K.E., Starling, A.P., Higgins, C.P., McDonough, C.A., Calafat, A.M., Adgate, J.L., 2020. Sociodemographic and behavioral determinants of serum concentrations of per- and polyfluoroalkyl substances in a community highly exposed to aqueous film-forming foam contaminants in drinking water. *Int. J. Hyg. Environ. Health*, 223(1), 256-266.

9. Bräunig, J., Baduel, C., Barnes, C.M., Mueller, J.F., 2019. Leaching and bioavailability of selected perfluoroalkyl acids (PFAAs) from soil contaminated by firefighting activities. *Sci. Total Environ.*, 646, 471-479.

10. Bräunig, J., Baduel, C., Heffernan, A., Rotander, A., Donaldson, E., Mueller, J.F., 2017. Fate and redistribution of perfluoroalkyl acids through AFFF-impacted groundwater. *Sci. Total Environ.*, 596-597, 360-368.

11. Buck, R.C., Franklin, J., Berger, U., Conder, J.M., Cousins, I.T., de Voogt, P., Jensen, A.A., Kannan, K., Mabury, S.A., van Leeuwen, S.P., 2011. Perfluoroalkyl and polyfluoroalkyl substances in the environment: terminology, classification, and origins. *Integr. Environ. Assess. Manag.*, 7(4), 513-41.

12. Choppin, G.R., Kullberg, L., 1978. Protonation thermodynamics of humic acid. *J. Inorg. Nucl. Chem.*, 40(4), 651-654.

13. Connolly, C.T., Cardenas, M.B., Burkart, G.A., Spencer, R.G.M., McClelland, J.W., 2020. Groundwater as a major source of dissolved organic matter to Arctic coastal waters. *Nature Comm.*, 11(1), 1479.

14. Corwin, C.J., Summers, R.S., 2011. Adsorption and desorption of trace organic contaminants from granular activated carbon adsorbers after intermittent loading and throughout backwash cycles. *Water Res.*, 45(2), 417-426.

15. Dalahmeh, S.S., Alziq, N., Ahrens, L., 2019. Potential of biochar filters for onsite wastewater treatment: Effects of active and inactive biofilms on adsorption of per- and polyfluoroalkyl substances in laboratory column experiments. *Environ. Pollut.*, 247, 155-164.

16. Dauchy, X., Boiteux, V., Colin, A., Hémard, J., Bach, C., Rosin, C., Munoz, J.-F., 2019. Deep seepage of per- and polyfluoroalkyl substances through the soil of a firefighter training site and subsequent groundwater contamination. *Chemosphere*, 214, 729-737.

17. Donat-Vargas, C., Bergdahl, I.A., Tornevi, A., Wennberg, M., Sommar, J., Kiviranta, H., Koponen, J., Rolandsson, O., Åkesson, A., 2019a. Perfluoroalkyl substances and risk of type II diabetes: A prospective nested case-control study. *Environ. Int.*, 123, 390-398.

18. Donat-Vargas, C., Bergdahl, I.A., Tornevi, A., Wennberg, M., Sommar, J., Koponen, J., Kiviranta, H., Åkesson, A., 2019b. Associations between repeated measure of plasma perfluoroalkyl substances and cardiometabolic risk factors. *Environ. Int.*, 124, 58-65.

19. Dontsova, K.M., Bigham, J.M., 2005. Anionic Polysaccharide Sorption by Clay Minerals. *Soil Sci. Soc. Am. J.*, 69(4), 1026-1035.

20. Du, Z., Deng, S., Chen, Y., Wang, B., Huang, J., Wang, Y., Yu, G., 2015. Removal of perfluorinated carboxylates from washing wastewater of perfluorooctanesulfonyl fluoride using activated carbons and resins. *J. Hazard. Mater.*, 286, 136-143.

21. Fang, L., Li, J.-s., Donatello, S., Cheeseman, C.R., Poon, C.S., Tsang, D.C.W., 2020. Use of Mg/Ca modified biochars to take up phosphorus from acid-extract of incinerated sewage sludge ash (ISSA) for fertilizer application. *J. Cleaner Prod.*, 244, 118853.

22. Gagliano, E., Sgroi, M., Falciglia, P.P., Vagliasindi, F.G.A., Roccaro, P., 2020. Removal of poly- and perfluoroalkyl substances (PFAS) from water by adsorption: Role of PFAS chain length, effect of organic matter and challenges in adsorbent regeneration. *Water Res.*, 171, 115381.

23. Goss, K.-U., 2008. The pKa Values of PFOA and Other Highly Fluorinated Carboxylic Acids. *Environ. Sci. Technol.*, 42(2), 456-458.

24. Guo, W., Huo, S., Feng, J., Lu, X., 2017. Adsorption of perfluorooctane sulfonate (PFOS) on corn straw-derived biochar prepared at different pyrolytic temperatures. *J. Taiwan Inst. Chem. E.*, 78, 265-271.

25. Hale, S.E., Arp, H.P.H., Slinde, G.A., Wade, E.J., Bjørseth, K., Breedveld, G.D., Straith, B.F., Moe, K.G., Jartun, M., Høisæter, Å., 2017. Sorbent amendment as a remediation strategy to reduce PFAS mobility and leaching in a contaminated sandy soil from a Norwegian firefighting training facility. *Chemosphere*, 171, 9-18.

26. Higgins, C.P., Luthy, R.G., 2006. Sorption of Perfluorinated Surfactants on Sediments. *Environ. Sci. Technol.*, 40(23), 7251-7256.

27. Jeon, J., Kannan, K., Lim, B.J., An, K.G., Kim, S.D., 2011. Effects of salinity and organic matter on the partitioning of perfluoroalkyl acid (PFAs) to clay particles. *J. Environ. Monit.*, 13(6), 1803-1810.

28. Korshin, G.V., Li, C.-W., Benjamin, M.M., 1997. Monitoring the properties of natural organic matter through UV spectroscopy: A consistent theory. *Water Res.*, 31(7), 1787-1795.

29. Kothawala, D.N., Köhler, S.J., Östlund, A., Wiberg, K., Ahrens, L., 2017. Influence of dissolved organic matter concentration and composition on the removal efficiency of perfluoroalkyl substances (PFASs) during drinking water treatment. *Water Res.*, 121, 320-328.

30. Kundu, S., Patel, S., Halder, P., Patel, T., Hedayati Marzbali, M., Pramanik, B.K., Paz-Ferreiro, J., de Figueiredo, C.C., Bergmann, D., Surapaneni, A., Megharaj, M., Shah, K., 2021. Removal of PFASs from biosolids using a semi-pilot scale pyrolysis reactor and the application of biosolids derived biochar for the removal of PFASs from contaminated water. *Environ. Sci.: Water Res. Technol.*, 7(3), 638-649.

31. Lin, P.-I.D., Cardenas, A., Hauser, R., Gold, D.R., Kleinman, K.P., Hivert, M.-F., Fleisch, A.F., Calafat, A.M., Webster, T.F., Horton, E.S., Oken, E., 2019. Per- and polyfluoroalkyl substances and blood lipid levels in pre-diabetic adults—longitudinal analysis of the diabetes prevention program outcomes study. *Environ. Int.*, 129, 343-353.

32. Liu, C.J., Werner, D., Bellona, C., 2019. Removal of per- and polyfluoroalkyl substances (PFASs) from contaminated groundwater using granular activated carbon: a pilot-scale study with breakthrough modeling. *Environ. Sci. Water Res. Technol.*, 5(11), 1844-1853.

33. Lu, D., Sha, S., Luo, J., Huang, Z., Zhang Jackie, X., 2020. Treatment train approaches for the remediation of per- and polyfluoroalkyl substances (PFAS): A critical review. *J. Hazard. Mater.*, 386, 121963.

34. Martin, M.J., Balaguer, M.D., Rigola, M., 1996. Feasibility of Activated Carbon Production from Biological Sludge by Chemical Activation with ZnCl2 and H2SO4. *Environ. Technol.*, 17(6), 667-671.

35. McCleaf, P., Englund, S., Östlund, A., Lindegren, K., Wiberg, K., Ahrens, L., 2017. Removal efficiency of multiple poly- and perfluoroalkyl substances (PFASs) in drinking water using granular activated carbon (GAC) and anion exchange (AE) column tests. *Water Res.*, 120, 77-87.

36. Mohan, D., Sarswat, A., Ok, Y.S., Pittman, C.U., 2014. Organic and inorganic contaminants removal from water with biochar, a renewable, low cost and sustainable adsorbent – A critical review. *Bioresour. Technol.*, 160, 191-202.

37. Murray, C.C., Vatankhah, H., McDonough, C.A., Nickerson, A., Hedtke, T.T., Cath, T.Y., Higgins, C.P., Bellona, C.L., 2019. Removal of per- and polyfluoroalkyl substances using super-fine powder activated carbon and ceramic membrane filtration. *J. Hazard. Mater.*, 366, 160-168.

38. Muvhiiwa, R., Kuvarega, A., Llana, E.M., Muleja, A., 2019. Study of biochar from pyrolysis and gasification of wood pellets in a nitrogen plasma reactor for design of biomass processes. *J. Environ. Chem. Eng.*, 7(5), 103391.

39. Nguyen, T.M.H., Bräunig, J., Thompson, K., Thompson, J., Kabiri, S., Navarro, D.A., Kookana, R.S., Grimison, C., Barnes, C.M., Higgins, C.P., McLaughlin, M.J., Mueller, J.F., 2020. Influences of Chemical Properties, Soil Properties, and Solution pH on Soil–Water Partitioning Coefficients of Per- and Polyfluoroalkyl Substances (PFASs). *Environ. Sci. Technol.*, 54(24), 15883-15892.

40. Oliver, D.P., Li, Y., Orr, R., Nelson, P., Barnes, M., McLaughlin, M.J., Kookana, R.S., 2020. Sorption behaviour of per- and polyfluoroalkyl substances (PFASs) in tropical soils. *Environ. Pollut.*, 258, 113726.

41. Park, M., Wu, S., Lopez, I.J., Chang, J.Y., Karanfil, T., Snyder, S.A., 2020. Adsorption of perfluoroalkyl substances (PFAS) in groundwater by granular activated carbons: Roles of hydrophobicity of PFAS and carbon characteristics. *Water Res.*, 170, 115364.

42. Phong Vo, H.N., Ngo, H.H., Guo, W., Hong Nguyen, T.M., Li, J., Liang, H., Deng, L., Chen, Z., Hang Nguyen, T.A., 2020. Poly- and perfluoroalkyl substances in water and wastewater: A comprehensive review from sources to remediation. *J. Water Proc. Eng.*, 36, 101393.

43. Rotander, A., Kärrman, A., Toms, L.-M.L., Kay, M., Mueller, J.F., Gómez Ramos, M.J., 2015. Novel Fluorinated Surfactants Tentatively Identified in Firefighters Using Liquid Chromatography Quadrupole Time-of-Flight Tandem Mass Spectrometry and a Case-Control Approach. *Environ. Sci. Technol.*, 49(4), 2434-2442.

44. Sammut, G., Sinagra, E., Sapiano, M., Helmus, R., de Voogt, P., 2019. Perfluoroalkyl substances in the Maltese environment – (II) sediments, soils and groundwater. *Sci. Total Environ.*, 682, 180-189.

45. Sasi, P.C., Alinezhad, A., Yao, B., Kubátová, A., Golovko, S.A., Golovko, M.Y., Xiao, F., 2021. Effect of granular activated carbon and other porous materials on thermal decomposition of per- and polyfluoroalkyl substances: Mechanisms and implications for water purification. *Water Res.*, 200, 117271.

46. Silvani, L., Cornelissen, G., Botnen Smebye, A., Zhang, Y., Okkenhaug, G., Zimmerman, A.R., Thune, G., Sævarsson, H., Hale, S.E., 2019. Can biochar and designer biochar be used to remediate per- and polyfluorinated alkyl substances (PFAS) and lead and antimony contaminated soils? *Sci. Total Environ.*, 694, 133693.

47. Singh, B., Macdonald, L.M., Kookana, R.S., van Zwieten, L., Butler, G., Joseph, S., Weatherley, A., Kaudal, B.B., Regan, A., Cattle, J., Dijkstra, F., Boersma, M., Kimber, S., Keith, A., Esfandbod, M., 2014. Opportunities and constraints for biochar technology in Australian agriculture: looking beyond carbon sequestration. *Soil Res.*, 52(8), 739-750.

48. Smebye, A., Alling, V., Vogt, R.D., Gadmar, T.C., Mulder, J., Cornelissen, G., Hale, S.E., 2016. Biochar amendment to soil changes dissolved organic matter content and composition. *Chemosphere*, 142, 100-105.

49. Sørmo, E., Silvani, L., Bjerkli, N., Hagemann, N., Zimmerman, A.R., Hale, S.E., Hansen, C.B., Hartnik, T., Cornelissen, G., 2021. Stabilization of PFAS-contaminated soil with activated biochar. *Sci. Total Environ.*, 763, 144034.

50. Wang, W., Mi, X., Zhou, Z., Zhou, S., Li, C., Hu, X., Qi, D., Deng, S., 2019. Novel insights into the competitive adsorption behavior and mechanism of per- and polyfluoroalkyl substances on the anion-exchange resin. *J. Colloid Interface Sci.*, 557, 655-663.

51. Wei, C., Wang, Q., Song, X., Chen, X., Fan, R., Ding, D., Liu, Y., 2018. Distribution, source identification and health risk assessment of PFASs and two PFOS alternatives in groundwater from non-industrial areas. *Ecotox. Environ. Safety*, 152, 141-150.

52. Wu, C., Klemes, M.J., Trang, B., Dichtel, W.R., Helbling, D.E., 2020. Exploring the factors that influence the adsorption of anionic PFAS on conventional and emerging adsorbents in aquatic matrices. *Water Res.*, 182, 115950.

53. Xiao, F., Jin, B., Golovko, S.A., Golovko, M.Y., Xing, B., 2019. Sorption and Desorption Mechanisms of Cationic and Zwitterionic Per- and Polyfluoroalkyl Substances in Natural Soils: Thermodynamics and Hysteresis. *Environ. Sci. Technol.*, 53(20), 11818-11827.

54. Xiao, X., Ulrich, B.A., Chen, B., Higgins, C.P., 2017. Sorption of Poly- and Perfluoroalkyl Substances (PFASs) Relevant to Aqueous Film-Forming Foam (AFFF)-Impacted Groundwater by Biochars and Activated Carbon. *Environ. Sci. Technol.*, 51(11), 6342-6351.

667 55. Xu, B., Liu, S., Zhou, J.L., Zheng, C., Weifeng, J., Chen, B., Zhang, T., Qiu, W., 2021. PFAS and their
668 substitutes in groundwater: Occurrence, transformation and remediation. *J. Hazard. Mater.*, 412, 125159.

669 56. Yong, Z.Y., Kim, K.Y., Oh, J.-E., 2021. The occurrence and distributions of per- and polyfluoroalkyl
670 substances (PFAS) in groundwater after a PFAS leakage incident in 2018. *Environ. Pollut.*, 268, 115395.

671 57. Yu, J., Lv, L., Lan, P., Zhang, S., Pan, B., Zhang, W., 2012. Effect of effluent organic matter on the
672 adsorption of perfluorinated compounds onto activated carbon. *J. Hazard. Mater.*, 225-226, 99-106.

673 58. Zhang, D., He, Q., Wang, M., Zhang, W., Liang, Y., 2019a. Sorption of perfluoroalkylated substances
674 (PFASs) onto granular activated carbon and biochar. *Environ. Technol.*, 1-12.

675 59. Zhang, D.Q., Zhang, W.L., Liang, Y.N., 2019b. Adsorption of perfluoroalkyl and polyfluoroalkyl substances
676 (PFASs) from aqueous solution - A review. *Sci. Total Environ.*, 694, 133606.

677 60. Zhang, W., Zhang, D., Liang, Y., 2019c. Nanotechnology in remediation of water contaminated by poly-
678 and perfluoroalkyl substances: A review. *Environ. Pollut.*, 247, 266-276.

679

680